THEMIS Ground-Based Magnetometers

**C.T. Russell · P.J. Chi · D.J. Dearborn · Y.S. Ge ·
B. Kuo-Tiong · J.D. Means · D.R. Pierce · K.M. Rowe ·
R.C. Snare**

Abstract The THEMIS mission includes a comprehensive ground-based measurement network that adds two additional dimensions to the information gained in the night magnetosphere by the five THEMIS spacecraft. This network provides necessary correlative data on the strength and extent of events, enables their onsets to be accurately timed, and provides an educational component in which students have an active participation in the program. This paper describes the magnetometers installed to obtain these ground-based North American magnetic measurements, including the magnetometers installed as part of the educational effort, and the support electronics provided by UCLA for the ground-based observatories. These magnetometers measure the Earth's magnetic field with high resolution, and with precise timing provided by the Global Positioning System. They represent UCLA's next generation of low-cost, ground-based magnetometers using an inexpensive personal computer for data collection, storage and distribution. These systems can be used in a stand-alone mode requiring only AC power. If there is Internet connectivity, they can be configured to provide near real-time data over the web. These data are provided at full resolution to the entire scientific community over the web with minimal delay.

Keywords THEMIS · Magnetometers · Ground-based magnetometer

1 Introduction

The underlying thesis of the THEMIS mission is that a combination of spatial information on the location and timing of events in the tail during substorms with complementary two-dimensional ground-based data at the feet of these field lines, will enable the location and time of onset of substorms to be identified, and the evolution of the disturbance to be

C.T. Russell (✉) · P.J. Chi · D.J. Dearborn · Y.S. Ge · B. Kuo-Tiong · J.D. Means · D.R. Pierce ·
K.M. Rowe · R.C. Snare
Institute of Geophysics and Planetary Physics, University of California, Los Angeles,
90095-1567 CA, USA
e-mail: ctrussel@igpp.ucla.edu

followed in space and time. This information will then be used to distinguish between competing models of substorms and other dynamical phenomena in the magnetotail. The auroral ionosphere is essentially a giant TV screen for THEMIS, a plasma screen if you will, that gives high definition pictures complementing the very coarse pixels available in space.

Both magnetometers and all-sky imagers (ASI) monitor this plasma screen. The imagers have the largest field of view outlining where electrons are accelerated down into the upper atmosphere. Twenty stations can provide nearly complete coverage over Canada and Alaska. Magnetometers sense the currents flowing in the auroral ionosphere at an altitude of close to 100 km. Thus magnetometers sense a region above them of only about 100 km in radius and not 500 km as the all-sky imagers do. Ideally it would be desirable to have instruments every 100 km. This would necessitate having the number of magnetometers be 25 times larger than the number of ASI's. However, a 500-site array is not affordable and some compromises must be made. Thus the magnetometer array is collocated with the all-sky-imager array to give coarse latitudinal and longitudinal data. It is crossed with several more finely spaced latitudinal chains, most notably CARISMA and its extension, McMAC and the Alberta Chain and its extension to the south. With these stations current intensifications should be resolvable to about 1° in latitude and 10º in longitude.

Accurate timing and high temporal resolution are very important for understanding the substorm onset. One needs to determine the time of the first acceleration, and one needs to be able to resolve rapidly oscillating phenomena such as Pi1B waves near 1 Hz. Thus GPS timing is used both for the imagers and the magnetometers and the magnetic field data are returned with a 2 Hz cadence.

Of the 50 states, only Alaska lies under the quiet-time auroral zone. However, many of the northern tier of the 48 contiguous states lie close enough to the auroral zone that under disturbed conditions both aurora and significant magnetic disturbances will be seen. Thus an education program was developed around the installation of magnetometers at 11 U.S. high schools. This allows the students to make a meaningful contribution to the science of THEMIS and participate with the THEMIS scientists in the excitement of the program.

In the sections that follow we describe the sensor that measures the magnetic signal; the electronics unit that powers the sensors and handles the data; the GPS timing circuit; the installation of the magnetometers; the data returned; and the plans for archiving the data.
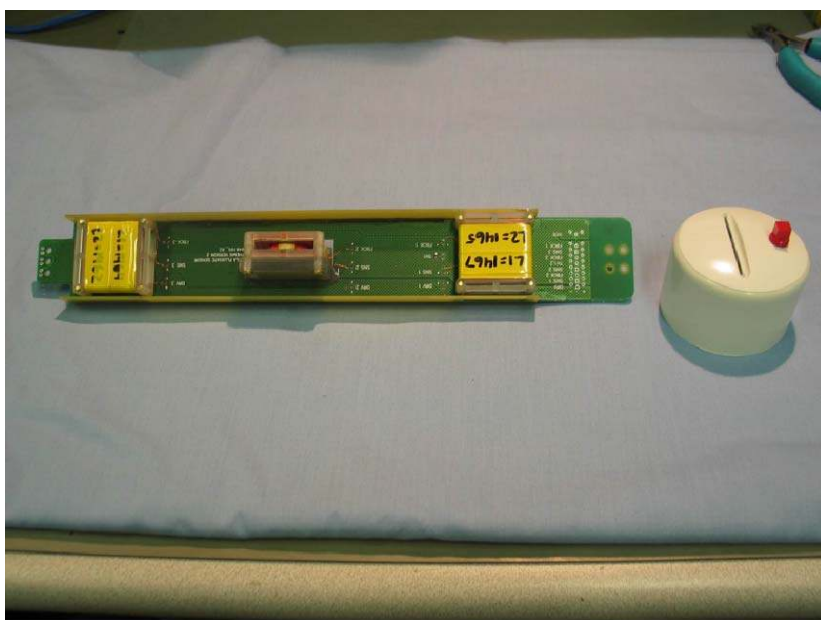
2 Magnetometer Sensor

The mechanical design of the sensor used in the ground-based magnetometers for the THEMIS mission is based on the successful design for the earlier Sino Magnetic Array at Low Latitudes (SMALL) terrestrial vector fluxgate magnetometer (Gao et al. 2000). Three single axis sensors are mounted on a printed circuit board in an orthogonal arrangement. Each of these three sensors is constructed, as shown in Fig. 1, on a one-inch diameter ring core wrapped with a multi-layer toroidal winding. This core is then slipped inside an outer solenoidal winding. The sense axis is aligned with the axis of the solenoid. Precise machining and winding of the solenoid and mounting fixture allow for orthogonality within 0.1°.

The printed circuit board fixture holding the set of three orthogonal sensors is reinforced with side stiffeners to ensure mechanical stability as shown in Fig. 2. It is assembled with a hermetically sealed 1.5-inch diameter white polyvinyl chloride (PVC) tube filled with paraffin oil to provide a stable thermal environment. Paraffin oil is chosen for its non-reactivity with the materials used in the construction of the fluxgate sensor as well as for its high thermal capacity. The right side of Fig. 2 shows the end cap of the white PVC tube containing a
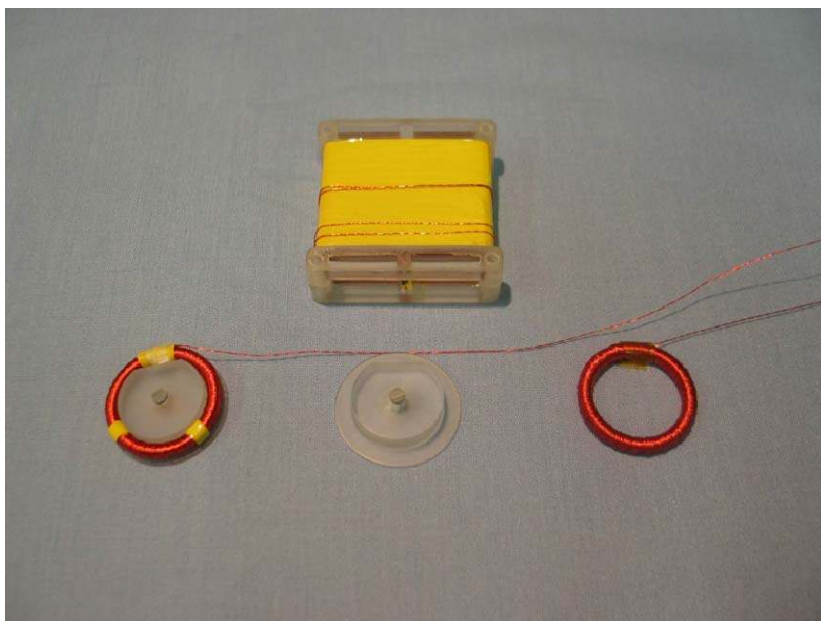
Fig. 1 THEMIS ground-based magnetometer sensor showing (*right*) toroidal winding on core and (*upper middle*) outer solenoidal winding into which core slips

Fig. 2 Printed circuit board fixture holding three orthogonal sensors (*right*). End cap of surrounding PVC tube has slit to allow end of circuit board to interface to cable

Fig. 3 Outer casing of magnetometer with 30-m cable covered by garden hose attached

slot through which the end of the printed circuit board extends. Electrical connections to the sensor triad are made directly to this portion of the printed circuit board. The board is then fastened with epoxy to the PVC tube end cap. A slotted disk (not shown) is fastened, again by epoxy into one end of the PVC tube. The sensor fixture has a protrusion that fits into the slotted disk ensuring proper axial alignment of the sensor in the tube. The fit between the slotted disk and the sensor fixture is left unglued to allow for slippage during any thermal expansion or contraction of the sensor fixture. In this way, the alignment of the sensor is maintained over a broad range of ambient temperatures.

A 30-meter cable, Belden type 8774 with nine shielded twisted pairs connects the sensor to the electronics chassis. Prior to assembly of the magnetometer, the 30-meter cable is encased in a 3/4 inch diameter common garden hose. This hose provides sufficient protection to the cable to allow it to be buried in the ground without the need for a special conduit.

The white PVC tube is then placed inside a larger four-inch diameter, 1.1-meter-long black PVC tube. Closed cell foam is installed between the walls of the white and the black PVC tubes for additional insulation. The black outer PVC tube is 0.5 meters longer than the inside white tube, allowing the sensor to be easily buried to greater depth. This provides both greater mechanical and greater thermal stability. Figure 3 shows the final assembled sensor ready to be installed. When installed, the sensor assembly is buried vertically in the ground with the top extending sufficiently above the ground to ensure that any standing water does not breach the top cap of the sensor.

A typical site installation is shown in Fig. 4. The PVC tube is vertically oriented and the cable buried. Once it is properly installed, the sensor assembly's thermal design ensures a stable environment for the three orthogonal fluxgate sensors. Temperature variations at the sensor are less than 20°C seasonally resulting in less than 2 nT seasonal offset error. Diurnal temperature changes are attenuated by 95%. Thus a site with a 20°C diurnal change external to the magnetometer would see a diurnal change of only 1°C at the sensor or less than 0.1 nT offset error over the diurnal cycle.

Fig. 4 Completed installation showing buried sensor housing and buried cable

3 Electronics and GPS Circuits

The THEMIS ground-based magnetometer has been designed to provide a cost-effective, high-resolution (10 pT), low-noise ($\pm$25 pTrms) vector measurement of the geomagnetic field at 2 Hz with a GPS-driven timing accuracy of better than 1 msec while being suitable for field deployment requiring a minimum of on-site attention. To achieve this level of performance, several design improvements have been made to UCLA's (SMALL) terrestrial vector fluxgate magnetometer. These include the incorporation of an innovative sigma-delta data processing technique eliminating the need for a precision high-resolution analog-to-digital converter, the addition of a programmable offsetting system capable of fully offsetting a 72k nT field in all three axis independently, and the combined use of a state-of-the-art GPS receiver and temperature-stabilized, crystal, local oscillator capable of assuring timing accuracy in the event of the loss of GPS signal. These elements are illustrated in Fig. 5.
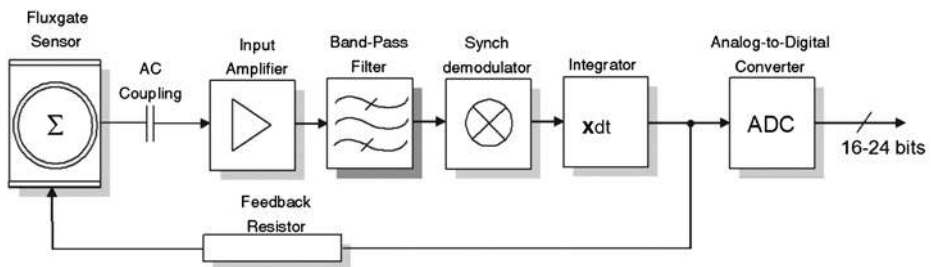
Traditionally, the fluxgate magnetometer electronics has been implemented using amplification, a bandpass filter, synchronous demodulator, integrator, feedback, and analog to digital converter (ADC) as shown in Fig. 6. In this design, a magnetic field is generated in the sense winding that counters the ambient field resulting in a zero-field environment within the sensor along the measurement axis. By operating the fluxgate sensor core in a zero-feedback field, a high degree of linearity is achieved. Two drawbacks of this design, however, are the need for a multi-pole bandpass filter and a precision ADC. Instability in the filter and the limited resolution of conventional ADC's limits the long-term stability and accuracy of the magnetometer in the geomagnetic field.

The use of the sigma-delta technique eliminates the need for these two components while preserving the performance of the fluxgate sensor. The architecture chosen is that of a second order sigma-delta modulator, illustrated in Fig. 7. Optimal performance is achieved by using the field canceling action of the fluxgate sensor in place of the input differencing element of the sigma-delta modulator input as shown in Fig. 8. The output of the modulator, shown
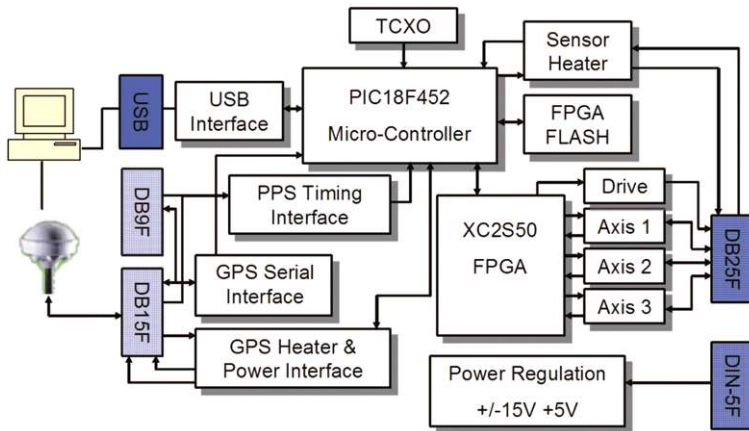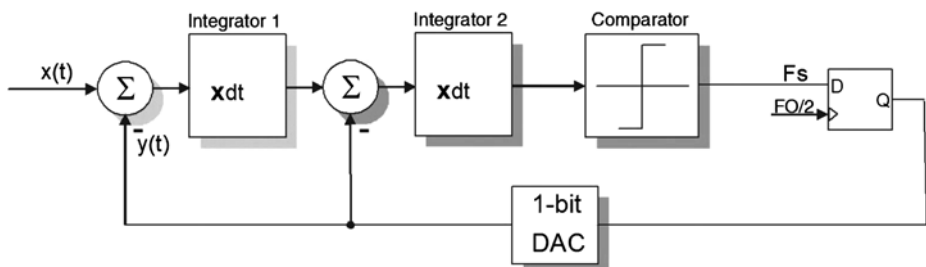
**Fig. 5** Functional block diagram of the fluxgate magnetometer

Fig. 6 Feedback circuit of traditional fluxgate magnetometer

Fig. 7 Functional block diagram of a second-order sigma-delta modulator used for analog-to-digital conversion

as Dout, is a serial bit stream. This bit stream has the characteristic that the density of logic high versus logic low is an accurate representation of the magnetic field. Furthermore, a desirable feature of the sigma-delta modulator is its digitization noise shaping characteristic (Magnes et al. 2003).

The serial bit stream is filtered by use of a comb filter comprised of a set of 4 integrators connected in series followed by a set of 4 differentiators in series as is standard practice for sigma-delta modulators for analog-to-digital converters. The output of this comb filter
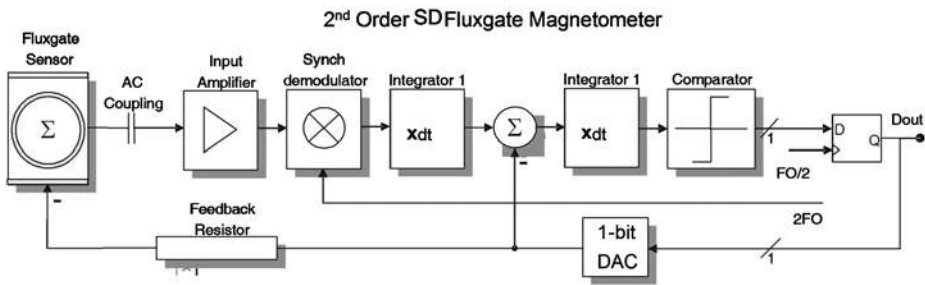
Fig. 8 Feedback circuit of a second-order sigma-delta fluxgate magnetometer

is decimated by a factor of 32, resulting in a 17-bit value at a data rate of 100 Hz. This 17-bit data stream is further filtered and decimated by 50 to reject the high-frequency digitization noise resulting in a 2 Hz data stream with 20-bit resolution and 1 Hz low-pass corner frequency. Figure 9 shows the time series and spectral output of the magnetometer in the presence of a 6 nT 0.2 Hz field applied to the vertical axis.

To achieve a resolution of 10 pT with 20 bits, the dynamic range of the sigma-delta modulator is limited to ±4,000 nT. In order to operate the magnetometer in the geomagnetic field of 72k nT, an offset system was employed. For ease of installation, a three-axis bipolar offset system has been implemented. This allows for each of the three axes of the magnetometer to offset the full geomagnetic field in either polarity. This feature facilitates installation in the southern hemisphere. To achieve this, a 3-channel DAC under the control of the data collection system has been configured to provide 128 offset field values in each polarity. Each step in field is approximately 550 nT in size. Under program control, the magnetometer can be commanded to automatically select the optimal offset field setting to provide maximum dynamic range within the sigma-delta loop of each axis. This need only be done during initial system installation. The value of the offset for each of the three magnetometer axis is recorded within the data stream so that the value of the geomagnetic field for each axis can be reconstructed.

Timing accuracy is obtained by combining the time of day accuracy of the Acutime-2000 GPS receiver with the long-term stability of a Vectron Series TC-400 temperature compensated crystal oscillator (TCXO). The combination of these two time sources allows for synchronization of data collection between magnetometers anywhere in the world. The Acutime 2000 GPS provides a 1 Hz strobe that is synchronized to occur at the zero millisecond boundary of every 1 second tic. When sufficient GPS satellite signals are present, this 1-second strobe is used to time tag the data processing logic within the magnetometer. The local oscillator derived from the Vectron TCXO is also periodically resynchronized to the GPS 1-second strobe. Each time this occurs, a measurement is obtained of the drift rate of the TCXO. These data are collected as a part of the overall GMAC data log stream. In the event that the GPS satellite signal is lost, the TCXO will free run allowing seamless data collection for an extended period of time. Without GPS satellite signal, the TCXO will be expected to drift at a rate of less than 0.2 seconds per day. This drift rate limits the duration in which synchronization of data sampling between stations can be maintained. The drift rate of the TCXO for each station is however well-known, due to the continual measurement of its drift relative to the GPS 1-second strobe. Therefore, time knowledge can be corrected to an uncertainty of less than 10 msec per day.
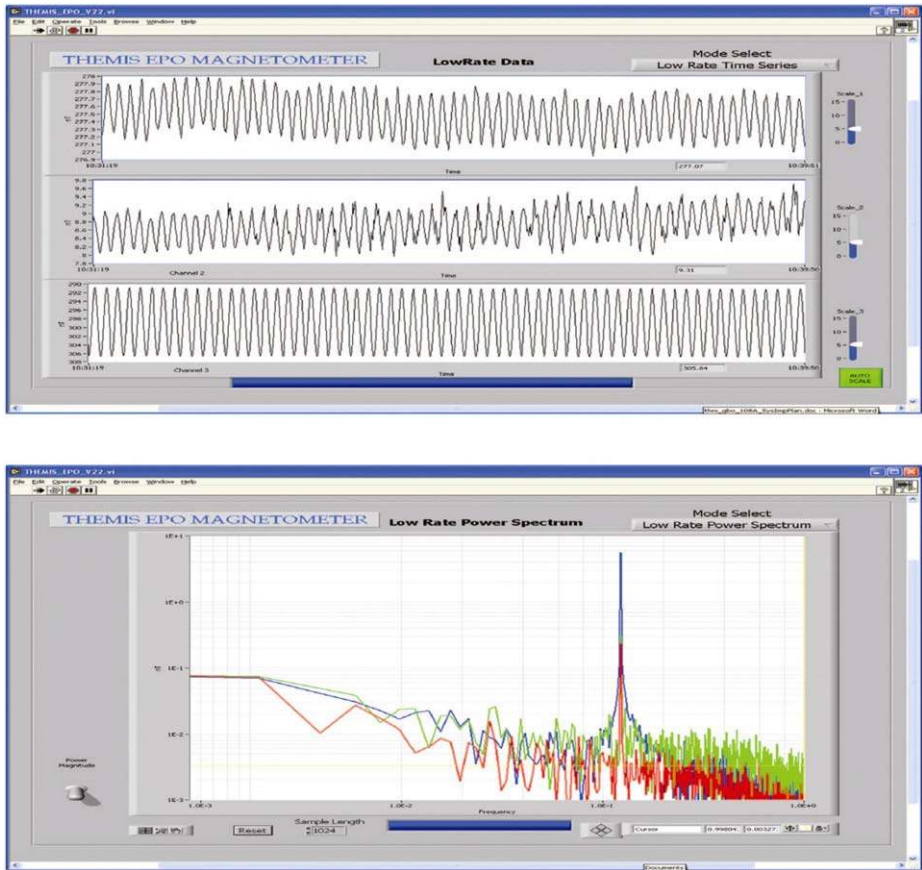
Fig. 9 Response of magnetometer to an applied 6 nT amplitude, 0.2 Hz frequency sinusoidal input. (*Top*) Eight minutes of time series in each of the three components. (*Bottom*) Amplitude spectrum on log–log scale from 10^{-3} to 1 Hz showing spectral peak at 0.2 Hz

4 Installation

The final configuration of the THEMIS ground magnetometer array consists of ten UCLA magnetometers installed with all-sky imagers at Canadian and Alaskan ground-based observatory (GBO) locations. Ten other Canadian all-sky camera sites already had magnetometers installed. Eleven further magnetometers in Alaska and in the contiguous states were installed in schools across the northern portion of the country. Only the Alaskan, Education and Public Outreach (EPO), site could be considered to be in the auroral zone but all were sufficiently sensitive to subauroral geomagnetic activity that they were useful both pedagogically and scientifically. The GBO magnetometers were installed by University of Calgary personnel. These sites have been described by Harris et al. (2008), and Mende et al. (2008). The EPO sites were installed by UCLA personnel. The THEMIS Education and Public Outreach program has been described by Peticolas et al. (2008).

The magnetometer system installed at the schools is shown disassembled in Fig. 10. This diagram shows the outer black PVC tube and its extension section on the right and left sides of the picture. The closed cell foam, the white PVC tube, the printed circuit board with

Fig. 10 Ground-based magnetometer sensor and electronics disassembled. On the *left* and *right* are segments of the exterior black PVC tube. The *grey* cylinder is the closed cell foam. The white PVC tube contains the sensors mounted on the printed circuit board. Next are the magnetometer electronics unit and the GPS electronics

Fig. 11 Magnetometer kit shipped to each EPO site. In *back row*, personal computer tower and monitor sit on shipping box. *To the left* is the cable encased in a garden hose. *In front* are the sensor, GPS system, UPS system, cords and cables

sensors, the electronics board and its housing are arrayed left to right across the picture. Completing the installation require the 30 m cable in a garden hose, a global positioning system (GPS), an uninterruptible power supply (UPS), a computer monitor and modem, and a shipping box as shown in Fig. 11. As shown in Fig. 12, the teachers and students assist

Fig. 12 Teacher and students at Remus assist with the installation of the magnetometer

in the installation of the magnetometers by helping dig the holes and test for aliveness of the magnetometers. The GPS unit provides precise timing for the magnetometers so that all units can be intercompared precisely. These units are generally installed on the roof of the facility as shown in Fig. 13.

The orbits of the THEMIS satellites are phased so that they come into alignment in the geomagnetic tail over North America. The longitudinal extent of auroral processes is large, typically 90° to 180° in extent. Thus it is important to have not only good latitudinal coverage, but good longitudinal coverage as well. Figure 14 shows the location of both the GBO and EPO magnetometers, and Table 1 lists the geographic location and magnetic coordinates of each station. While the data from these 21 sites are collected daily and provided to the THEMIS community, many more sites are providing high cadence magnetic field measurements that will ultimately be available for use by the community, many available already. The full array of sites is shown in Fig. 15.

5 Data Management and Dissemination

The UCLA magnetic observatory consists of four components, the sensor, the GPS receiver, the magnetometer electronics unit and the PC based suite of software. The PC software is designed to facilitate the setup of the magnetometer, monitor the performance and health of the instrument, collect, archive and distribute the magnetometer data products and provide for remote access to the observatory over the Internet.

In most of the installations the software is designed to operate in a Microsoft Windows OS (XP Home) environment. The primary software component is implemented in LabView.

Fig. 13 Antenna for Global Positioning System signal acquisition installed on roof of facility in which magnetometer electronics is housed
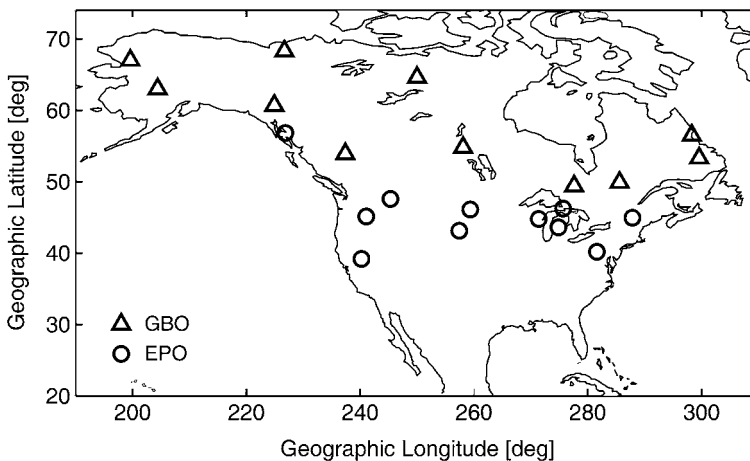
Fig. 14 Locations of GBO and EPO magnetometers

This application allows for setup of the magnetometer and the GPS unit, monitoring the real time data from the magnetometer both in time series and spectral density formats, monitoring the temperatures of the GPS receiver and the magnetometer electronics and sensor, and control of the data products.

There are two types of data products produced by the software, data files stored on the PC and real time data packets transmitted over the Internet. There are three types of data files created and stored on the PC, 'RMD', 'HKP' and 'LOD' files. The 'RMD' files contain the

Table 1 Location of the GBO and EPO magnetometers

Station (Code)	Geogr. lat. (deg)	Geogr. long. (deg)	MAG lat. (deg)	MAG long. (deg)	L	Inv. lat. (deg)	CGM long. (deg)
GBO							
Chibougamau (CHBG)	49.9	285.6	59.9	356.7	3.92	59.7	3.7
Fliti Flon (TPAS)	54.8	258.1	63.0	320.3	5.18	63.9	322.2
Goose Bay (GBAY)	53.3	299.6	63.0	15.2	4.18	60.7	23.2
Inuvik (INUV)	68.3	226.7	70.9	271.9	9.64	71.2	275.7
Kapuskasing (KAPU)	49.4	277.6	59.2	346.5	3.95	59.8	351.8
Kiana (KIAN)	67.0	199.6	65.1	248.8	5.67	65.2	253.5
Kuujjuarapik (KUUJ)	55.3	282.3	65.2	352.0	5.66	65.1	359.2
Lac de Gras (EKAT)	64.6	250.0	71.4	303.2	10.5	72.1	306.8
McGrath (MCGR)	63.0	204.4	62.2	256.6	4.47	61.8	259.8
Prince George (PGEO)	53.9	237.4	59.3	296.3	3.83	59.3	295.9
White Horse (WHIT)	60.7	224.9	63.7	278.3	4.98	63.4	279.4
EPO							
Bay Mills (BMLS)	46.24	275.66	55.92	344.48	3.33	56.8	348.9
Carson City (CCNV)	39.19	240.22	45.35	304.84	2.00	45.0	303.5
Derby (DRBY)	44.95	287.87	54.93	359.67	2.97	54.5	6.4
Fort Yates (FYTS)	46.09	259.35	54.54	324.71	3.12	55.5	325.5
Hot Springs (HOTS)	47.59	245.34	54.31	307.96	2.98	54.6	307.2
Loysburg (LOYS)	40.17	281.62	50.08	352.21	2.48	50.6	357.2
Petersburg (PTRS)	56.83	226.84	60.33	283.11	3.98	59.9	283.3
Pine Ridge (PINE)	43.11	257.40	51.39	323.14	2.67	52.3	323.3
Remus (RMUS)	43.60	274.84	53.25	343.78	2.92	52.2	347.6
Shawano (SWNO)	44.78	271.40	54.24	339.46	3.09	55.3	342.6
Ukiah (UKIA)	45.13	241.07	51.30	304.02	2.55	51.2	302.9

Raw Magnetometer Data. Each 'RMD' file contains one hour's worth of raw, unprocessed data from the electronics unit along with timing (accurate to 1ms) and station identification information. Each file takes up $\sim$ 104 kilobytes disk space. The 'HKP' files contain temperature, offset DAC values and a status byte from the GPS receiver, one record per minute for an entire day. Each 'HKP' file takes up $\sim$345 kilobytes. The 'LOD' files contain log data recording magnetometer configuration data, GPS status changes, and 'RMD' file creation and closing. Each 'LOD' file contains log data for one day and takes up $\sim$ 103 kilobytes of disk space. The sum of the disk space required for 'RMD', 'HKP' and 'LOD' files over one year is slightly greater than 1 Gbyte. A typical PC used for the installation will have approximately 40 Gbytes free space on hard drive at time of installation. The PC's are equipped with DVD R/W optical drives for local extraction of data archives.

The second type of data product produced by the software are the 'real time' data packet datagrams transmitted over the Internet. The protocol used is 'User Datagram Protocol' (UDP). Unlike TCP/IP protocol, UDP is connectionless, i.e. no response from the client is required or expected. This frees the server software from waiting for a 'packet received'
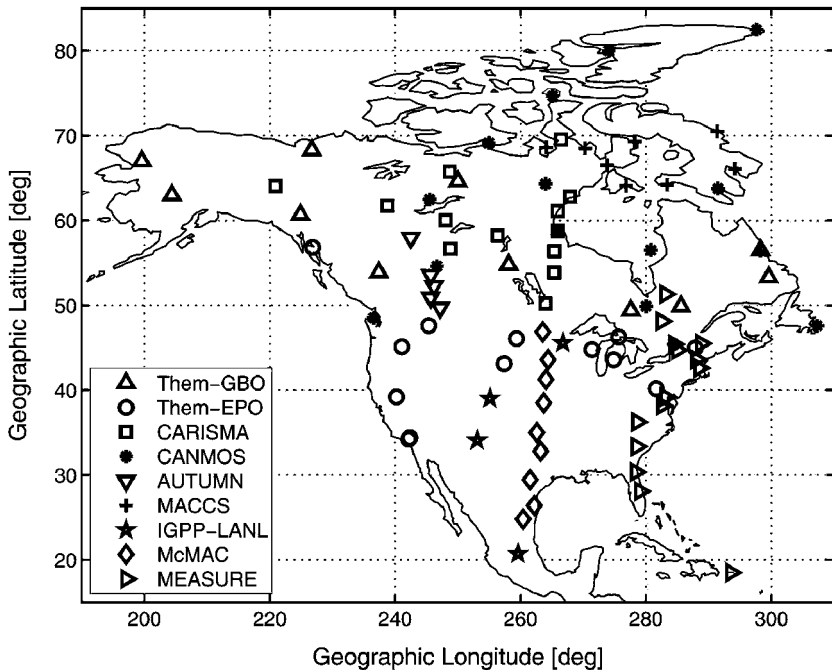
Fig. 15 Locations of ancillary magnetometers in North America together with two THEMIS arrays

acknowledgment from the client. Loss of Internet connection or a bottle neck slowing down transmission will have no effect on the server software. To improve chances of reception, all packets are kept to <512 bytes to preclude the packets being broken up when transmitted over media unable to accommodate packets >512 bytes.

Each mag data packet contains project and site identification strings (ProjID & SiteID), a datagram count number (DGC—incrementing by one for each packet transmitted to a client), temperatures of the magnetometer, sensor and GPS unit, GPS status, data timing information accurate to 1 ms, and up to 50 vectors of 2sps magnetic field data. These packets are transmitted every 5 seconds with a 20 second overlap. Under normal circumstances most data is received with no more than 5 seconds latency resulting in the client being able to present an almost 'real time' time series plot. The 20 second overlap means that most of the time, four consecutive datagrams would have to be lost in order to have a loss of data.

Experiments with a magnetometer installation at a remote site transmitting to a client at UCLA showed that over a 24 hour period ∼80% percent coverage of the data was achieved using this method. Running the same test with the client at a remote site resulted in ∼98% coverage, implying that most of the Internet bottle necks occur at UCLA. The GMAG software is capable of duplicating the UDP transmission to up to three different clients. By having the clients then retransmit the datagrams received to the other two clients who then discard datagrams received with identical SiteID, ProjID and DGC, almost 100% coverage can be achieved. This is accomplished with ∼3 packets of <512 bytes every 5 seconds resulting in a bandwidth requirement of ∼2400 bps.

In addition to the magnetometer data packets, log packets containing Project ID, site ID, DGC, time, date, magnetometer offset and scale values, transformation matrix, temper-

ature conversion coefficients, observatory latitude and longitude and any new information added to the LOD file at the observatory. These packets are also <512 bytes long and are transmitted every 5 minutes, whenever the log buffer is full or the configuration information changes. Under normal circumstances, no more that one log packet is transmitted every 5 minutes having little effect on bandwidth requirements.

The primary purpose of this UDP data product is real time data presentation both as a teaching tool at the EPO sites (a teacher can have a magnetometer UDP client running on classroom PC) and as a quick check by UCLA personnel on the health of all observatories currently operated by UCLA. A secondary purpose of the UDP packets is to duplicate the 'RMD', 'HKP' and 'LOD' files at UCLA in 'real time'. While a secure shell link (SSH) is setup on each observatory computer for downloading via RSYNC (a public domain database synchronization system), RSYNC will only transmit those portions of the database that are different. If 'RMD,' etc. files can be created 'real time' at the server, then once a day when RSYNC is scheduled to run very little data will need to be retransmitted, further reducing the observatory bandwidth requirements.
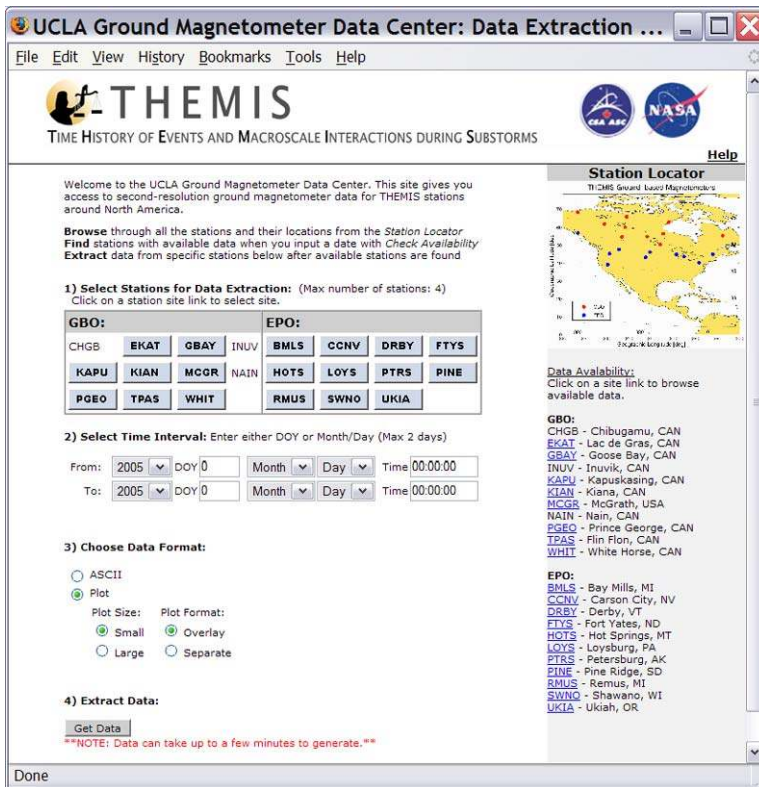
Each observatory has CYGWIN (a public domain LINUX 'look alike' that runs under Windows) installed with the SSH option. This allows engineering personnel to access the observatories remotely while keeping the holes in the local (to the observatory) firewall to a minimum. Remote access includes RSYNC, mentioned above, and VNC (public domain software implementing a virtual terminal) to allow the engineer to remotely upgrade software, change configuration parameters and diagnose and correct problems.

Each site also has an iBoot device that monitors a heart beat signal sent out by the magnetometer software over the local area network (LAN). The heartbeat signal should be sent once every 5 seconds. If the iBoot has not received a heartbeat in 10 minutes, it will power cycle the computer, magnetometer and electronics GPS. The iBoot has a password secured website built in that can be accessed by engineers at UCLA for configuration and manual power cycling of the PC, etc.

Each site also has an uninterruptible power supply (UPS) capable of running the observatory for ∼1 hour during AC power outages. The UPS interface software on the computer monitors the condition of the AC power and the status of the UPS batteries and automatically notifies the engineering staff at UCLA of changes.

Data products from the THEMIS EPO sites are updated daily, using RSYNC and are published at UCLA. Data Products from the THEMIS GBO sites are updated daily by UCB and Calgary. All magnetometer data, 'RMD', 'HKP' and 'LOD' files, both EPO and GBO are then 'mirrored' at UCLA, UCB and Calgary, again using RSYNC, insuring that complete databases are available at all three institutions. In addition, at UCLA, a website is available where magnetometer data is published in corrected ASCII format upon request.

The GBO observatories, in addition to the magnetometers also support the all-sky camera developed and built at UCB. The needs of this system dictated that a version of the magnetometer software be developed to run under Linux with a minimal impact on computer resources. The data product capabilities of the LabView software were duplicated in a software package written in 'C'. The 'RMD', 'HKP' and 'LOD' files created and UPD packets transmitted are the same as those produced by the LabView software, but without the graphical user interface provided by LabView. The LabView software is still used to setup and configure the magnetometer, then the configuration data is saved in an 'ini' file and the 'C' version of the magnetometer software is started as background task that runs with very little impact on the UCB provided software. UCB maintains and operates the GBO sites and collects the magnetometer and camera data.

Fig. 16 THEMIS ground magnetometer data center at UCLA (URL: http://www-ssc.igpp.ucla.edu/uclamag/themis_center/)

6 Web-Based Data Server

The THEMIS ground magnetometer data are available to the public through a dedicated online server at http://www-ssc.igpp.ucla.edu/uclamag/themis_center/. The front page of the data server is shown in Fig. 16. Users can either plot or download the data in the ASCII format in the selected time interval. When the plot function is selected, one plot can show data from up to four stations at the same time. When the ASCII data mode is chosen, the data listing includes a header that shows the essential attributes of the data, such as the time interval and calibration values of the magnetometer. The data server has a simple, straightforward user interface. A help file is also linked with the front page, explaining each step of the data extraction in detail.

7 Scientific Return

The THEMIS ground-based magnetometers have been providing high-quality data for scientific research since their installation in the years leading up to launch. Thus they were ready for action as soon as the instruments on THEMIS began taking data. For substorm studies, the prime objective of THEMIS, high-resolution geomagnetic field measurements provide
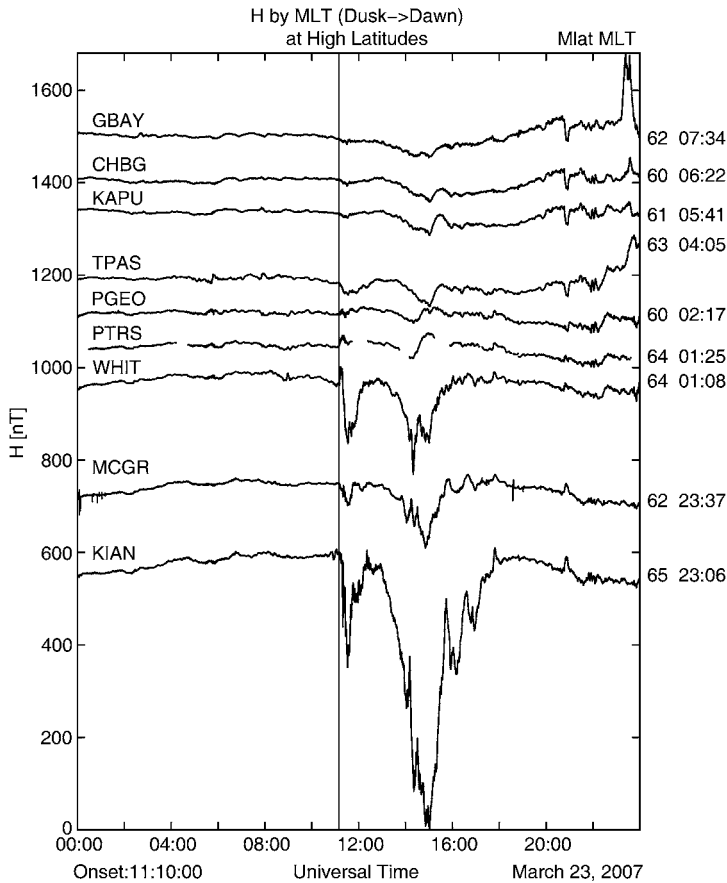
Fig. 17 *H*-component magnetograms for high latitude stations during the first THEMIS substorm event, on March 23, 2007

accurate information on substorm timing. At the expansion onset of substorms, the substorm current wedge (SCW) forms. The initial generation of this 3-D current system including the ionospheric electrojet and field-aligned currents (FACs) can be observed by ground-based magnetometers. The auroral stations (high-latitude stations) provide measurements which detect the variations of ionospheric currents, especially the westward electrojet at the expansion phase of substorms, while the magnetic field perturbations caused by FACs then are detected by the mid-latitude magnetometers. Below we show an example of how the magnetometers document the changing ionospheric currents and their locations during substorms, and the timing of substorm events with Pi1 and Pi2 waves.

Figure 17 shows the *H* components of geomagnetic field for high-latitude stations during the first THEMIS substorm event with conjugate observations and which has been studied comprehensively. The substorm onset is near 11:10 UT (the vertical line in Fig. 17) on March 23, 2007 (McPherron et al. 2008), when the THEMIS spacecraft constellation is located in the dusk–premidnight sector and all spacecraft are within the near-tail region at this time. Dipolarizations of the near-Earth tail magnetic field have been observed by all THEMIS spacecraft. At the same time, the images of aurora during this substorm are recorded by the
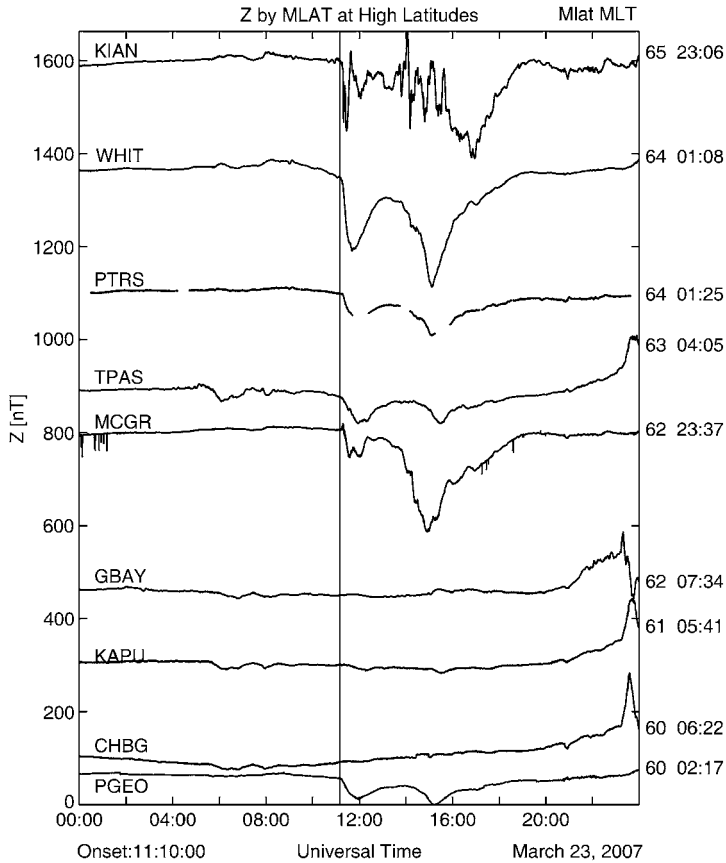
Fig. 18 Z-component magnetograms for high latitude stations during the March 23, 2007 substorm

Polar spacecraft in the southern hemisphere and also by the ground all-sky imagers at Fort
Yukon and Kiana (KIAN). In Fig. 17, sharp decreases of H components appear on White-
horse (WHIT) and KIAN at the substorm onset, showing that the westward electrojet forms
over these stations close to the magnetic local time (MLT) of 2300. The magnitude of the
largest decrease of H component at this onset is about 250 nT at KIAN (2306 MLT). Weaker
negative perturbations appear on the further east stations. The H component perturbations
indicate that this substorm is a moderate substorm comparing the following one which has
the maximum perturbation of 500 nT at around 1255 UT. The westward electrojet is located
at the premidnight sector and close or above the latitudes of KIAN (65°) and WHIT (64°).
The latitude of the westward electrojet can be inferred from the perturbations of Z com-
ponents at the onset which is shown in Fig. 18. The stations are ordered by their magnetic
latitudes in this figure from high to lower latitudes. All stations north of Goosebay (magnetic
latitude 62°) record negative perturbations in Z components, suggesting that the westward
electrojet forms at a higher latitude than this magnetometer network during this substorm.

The middle-latitude stations (the EPO chain) record the perturbations generated by the
FACs of the substorm current wedge (SCW) at the substorm onset. During the substorm,
the H components of mid-latitude stations are usually enhanced when the stations are lo-
cated within the sectors of the SCW, which is called a 'mid-latitude positive bay.' In this
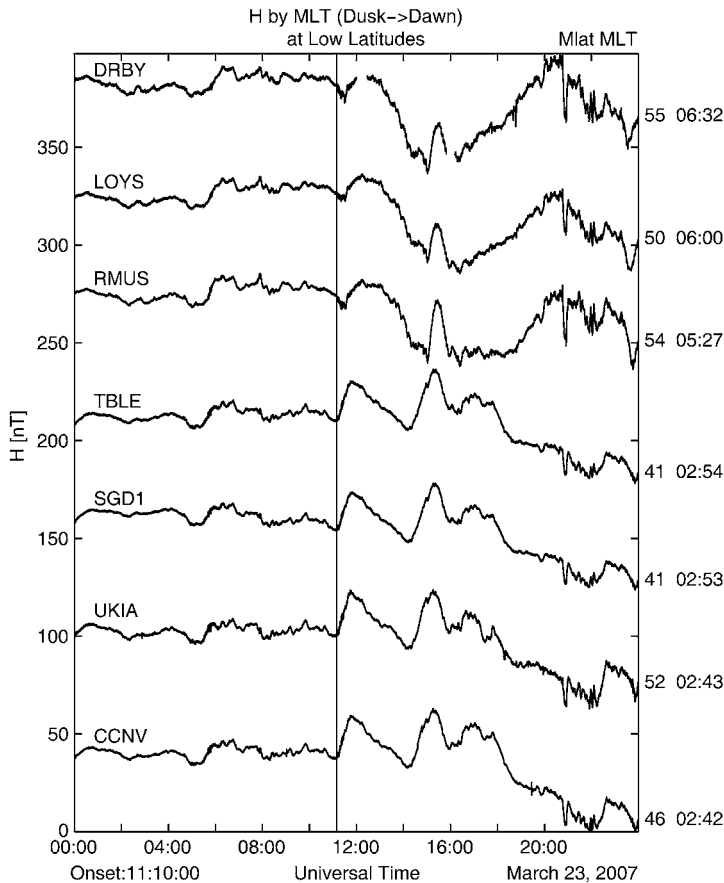
Fig. 19 *H*-component magnetograms from the EPO stations during the March 23, 2007 substorm

event, clear positive *H* bays are shown in Fig. 19 at the onset. The azimuthal expansion of SCW is also signaled by the shifting of positive bays on the stations further east. The *D* component perturbations in Fig. 20 indicate that all THEMIS EPO stations are located east of the SCW central meridian because all perturbations are negative (westward), which is caused by the downward FAC in space. Thus, high-latitude and mid-latitude stations detect the formation and expansion of the SCW at the onset. They also find that the westward electrojet is at a latitude higher than 65° and that on the onset, the SCW central meridian is west of Carson City (CCNV) at 0242 MLT.

For the timing of substorm onsets, ground Pi2 pulsations are generally used, but in this frequency band (40–150 seconds), the uncertainty of the timing is around half minutes (a quarter of typical period). Thus the higher-frequency wave-like pulsations in Pi1 band have been proposed to provide the more precise timing. The association of Pi1 bursty pulsations (Pi1 B) with substorm onsets was proposed in some early studies (e.g., Boesinger et al. 1981) and has been statistically investigated by Ge et al. (2007). It has been found that the Pi1 B pulsations generally appear at substorm onsets but can be detected only in a limited local time range, which can make them less generally useful than Pi2 pulsations (Ge et al. 2007).
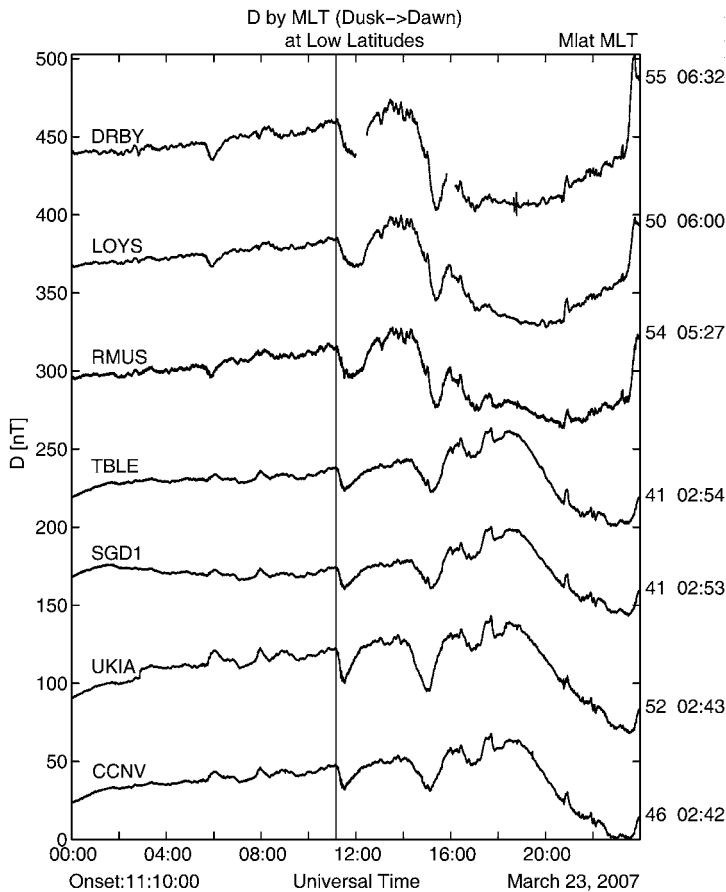
Fig. 20 *D*-component magnetograms from EPO stations during the March 23, 2007 substorms

The band-pass filtered *H* components in Pi1 and Pi2 bands are respectively shown in Figs. 21a and 21b. The Pi2 pulsation onsets are seen at all high-latitude stations but Pi1 B onsets are clear at only three stations (KIAN, McGrath, WHIT), demonstrating the localization of Pi1 B pulsations. The filtered *H* components for the mid-latitude EPO stations are shown in Figs. 22a and 22b. No clear Pi1 B onset is found on any mid-latitude stations while all stations record pulsations in Pi2 band Ge et al. (2007) shows that there is a considerable number of events in which Pi1 B pulsations appear also on mid-latitude stations. The authors believe that the absence of Pi1 B at mid-latitude stations in this event is due to the localization of Pi1 B because the MLT of the station (CCNV) which is the closest EPO station to the SCW central meridian is still 0242 at the substorm onset.

The apparent time delay among high-latitude stations for both Pi2 and Pi1 B pulsation onsets (Fig. 22) indicates that these pulsations are associated with the currents generated at the substorm onset and propagating azimuthally as the SCW expands. However, the Pi2 onsets on the mid-latitude EPO stations appear quite close to each other and are apparently later than the Pi2 onsets at high-latitude stations, suggesting that in the magnetosphere, Pi pulsations propagating inward from the tail, which gives the earlier onsets at high-latitude

Pi1 Band Filtered H by MLT
(Dusk→Dawn) at High Latitudes
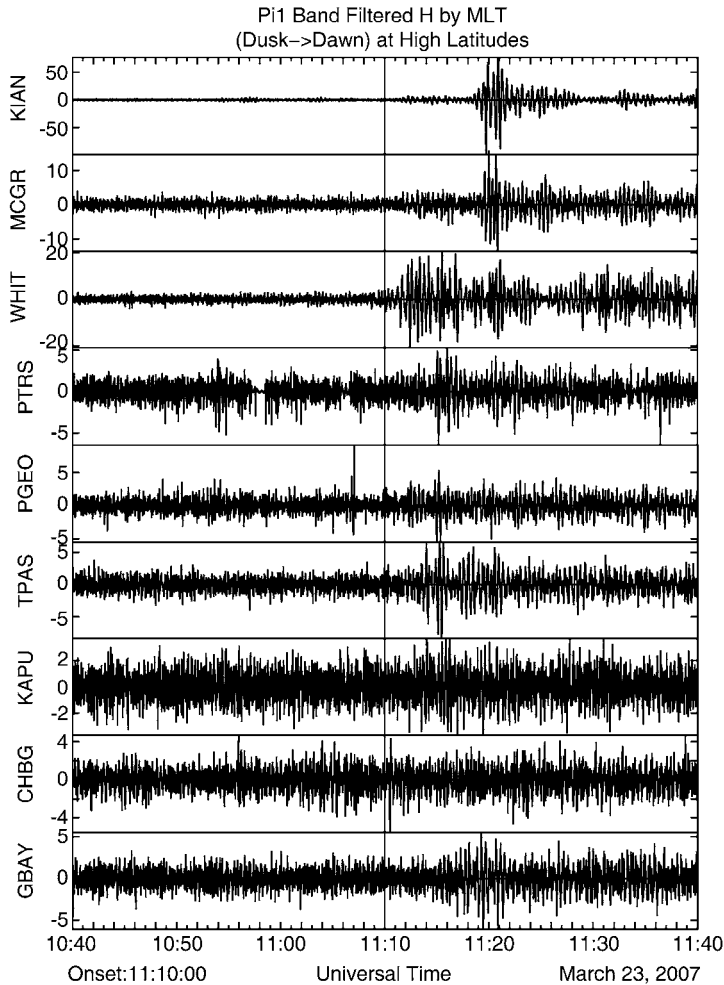
Fig. 21a Bandpass-filtered high-latitude magnetograms covering the Pi1 frequency band

stations. As they propagate closer to the Earth, they more likely become cavity-mode wave to give the almost simultaneous Pi2 onsets at mid-latitude stations.

The earliest onsets both in Pi1 and Pi2 bands are found at WHIT and close to the substorm onset time determined by McPherron et al. (2008) with more ground stations. The Pi2 onsets is more and more delayed as the station is further away from WHIT showing the clear propagation of signals as the expansion of SCW. According the Pi2-band filtered data on WHIT, the onset can be determined between the minima before the vertical line 11:09:00 and the later peak 11:10:20. The uncertainty of timing using Pi2 pulsations is inevitably from half minutes to even one minute. However, the determination from Pi1 B pulsations is more precise. Similar to the method for Pi2, the times for the minima and peak of the wave cycle closest to the Pi1 B onset are found at 11:10:58 and at 11:11:12. The uncertainty then comes down to about 7 seconds, much smaller than the uncertainty from the Pi2 timing. We note that the Pi1 B onset time in this event is about 30 seconds to one minute later than the Pi2 onset time and close to the mid-latitude Pi2 onset time, consistent with the statistical
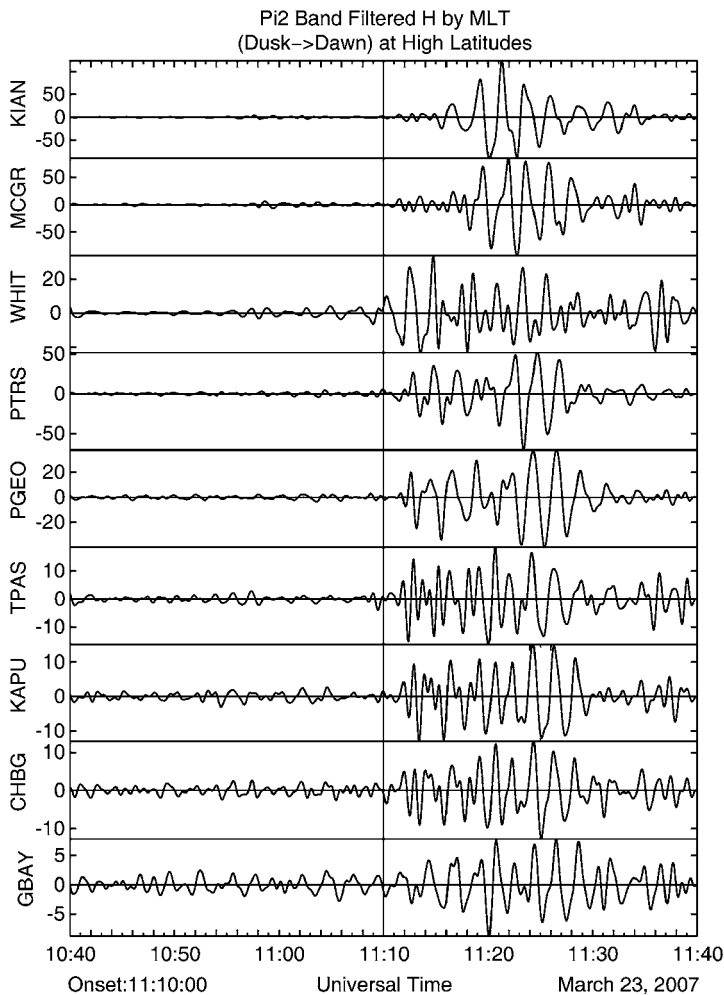
**Fig. 21b** Bandpass-filtered high-latitude magnetograms covering the Pi2 frequency band

results by Ge et al. (2007). Thus the Pi1B and the Pi2 waves are responding to different parts of the substorm onset and the relative accuracy of the two techniques may be a moot point.

8 Summary

The THEMIS ground-based magnetometers are installed and operating. Their design and operation represent an advance in the state-of-the-art scientific magnetometry. Costs have been minimized to enable the installation of extensive networks. Their operation has been kept simple so they can be operated remotely and reliably for long periods. They are quite appropriate to simultaneously act as a teaching device to introduce students to science and at the same time provide high-quality scientific data. Already the magnetometers are proving their worth, pointing accurately to both the location and the time of substorm onsets.
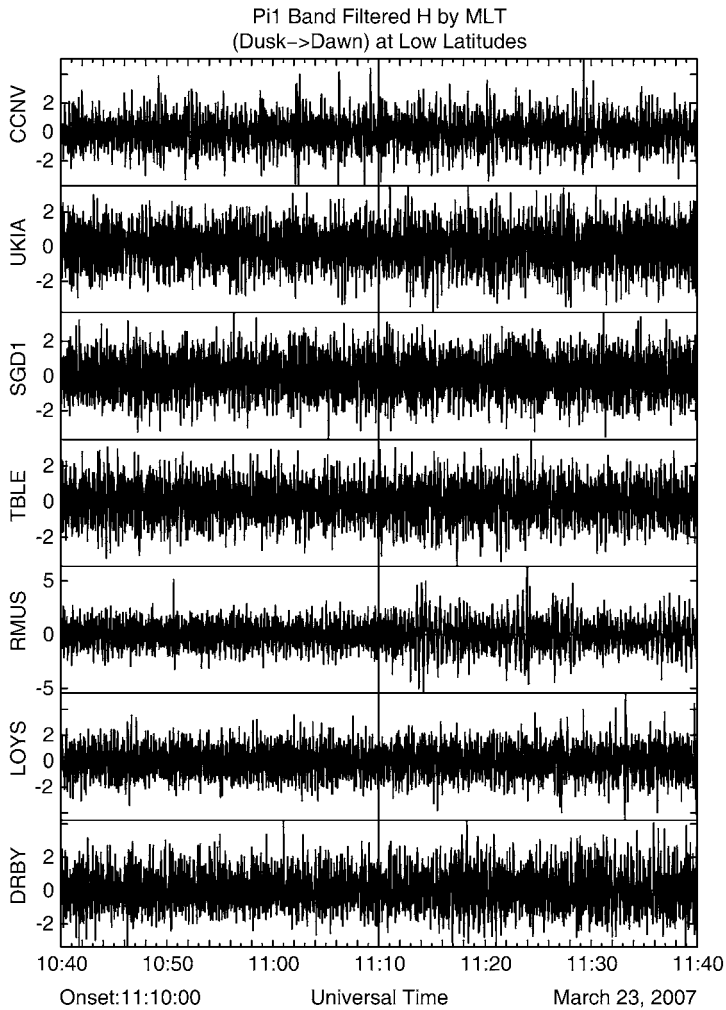
Fig. 22a Bandpass-filtered *H*-component magnetograms in the Pi1 range for EPO stations
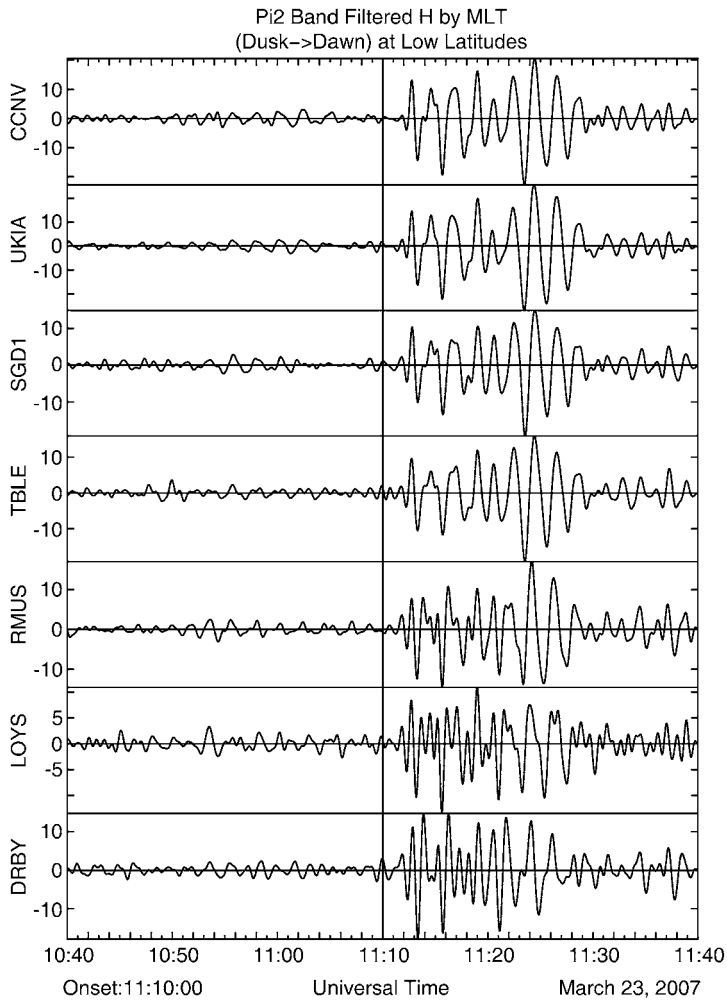
Fig. 22b Bandpass-filtered *H*-component magnetograms in the Pi2 range for EPO stations

References

T. Boesinger, K. Alanko, J. Kangas, W. Baumjohann, H. Opgenoorth, Correlations between PiB type magnetic micropulsations, auroras and equivalent current structures during two isolated substorms. J. Atmospheric Terr. Phys. **43**, 993–945 (1981)

Y.F. Gao, P.J. Chi et al., Sino-Magnetic Array at Low Latitudes (SMALL) including initial results from the sister sites in the United States. Adv. Space Res. **25**(7/8), 1343–1351 (2000)

Y.S. Ge, C.T. Russell, T.-S. Hsu, S. Mende, V. Angelopoulos, J.I. Rae, R.L. McPherron, Investigation on Pi1 B pulsations using THEMIS ground-based magnetometers. American Geophysical Union, Fall Meeting, 2007

S.E. Harris, S.B. Mende, V. Angelopoulos, W. Rachelson, E. Donovan, B. Jackel, M. Greffen, C.T. Russell, D. Pierce, D. Dearborn, THEMIS ground-based observatory system design. Space Sci. Rev. (2008, this issue)

W. Magnes, D. Pierce et al., A sigma-delta fluxgate mangnetometer for space applications. Meas. Sci. Technol. **14**, 1003–1012 (2003)

R.L. McPherron, V. Angelopoulos et al., Pi 2 timing of substorm expansion onset using THEMIS ground based observations and other data. Geophys. Rev. Lett. (2008, submitted)

S.B. Mende, S.E. Harris, H.U. Frey, V. Angelopoulos, E. Donovan, B. Jackel, M. Greffen, C.T. Russell, L.M. Peticolas, Space Sci. Rev. (2008, this issue)

L.M. Peticolas, N. Craig et al., The Time History of Events and Macroscale Interactions during Substorms (THEMIS) education and public outreach program. Space Sc. Rev. (2008, this issue)